Eur J Vasc Endovasc Surg (2020) 59, 237–246

Patient Specific Computer Modelling for Automated Sizing of Fenestrated Stent Grafts

Lucie Derycke [a,b,*], Jean Sénémaud [b], David Perrin [c], Stephane Avril [a], Pascal Desgranges [b], Jean-Noel Albertini [d], Frederic Cochennec [b], Stephan Haulon [e]

[a] Mines Saint-Etienne, Univ Lyon, Univ Jean Monnet, INSERM, U 1059 Sainbiose, Centre CIS, F – 42023 Saint-Etienne, France
[b] Department of Vascular Surgery, Henri Mondor Hospital, University of Paris XII, Créteil, France
[c] PrediSurge, 3, Saint-Etienne, France
[d] Department of Cardio-Vascular Surgery, Centre Hospitalier Régional Universitaire de Saint-Etienne, Saint-Priez-en-Jarez, France
[e] Department of Aortic and Vascular Surgery, Marie Lannelongue Hospital, Le Plessis-Robinson, INSERM UMR_S 999, Université Paris Sud, France

WHAT THIS PAPER ADDS

Fenestrated stent grafting has become a standard endovascular approach to treat complex abdominal aortic aneurysms. Currently, accurate device planning requires significant operator experience and a long manufacturing delay. This step is known to be crucial for surgical success. Computational modelling could prove helpful in providing more tailored and straightforward care in patients, especially for planning. This study explores the potential of simulation for fenestrated stent graft sizing.

Objective: The aim was to validate a computational patient specific model of Zenith® fenestrated device deployment in abdominal aortic aneurysms to predict fenestration positions.

Methods: This was a retrospective analysis of the accuracy of numerical simulation for fenestrated stent graft sizing. Finite element computational simulation was performed in 51 consecutive patients that underwent successful endovascular repair with Zenith® fenestrated stent grafts in two vascular surgery units with a high volume of aortic procedures. Longitudinal and rotational clock positions of fenestrations were measured on the simulated models. These measurements were compared with those obtained by (i) an independent observer on the post-operative computed tomography (CT) scan and (ii) by the stent graft manufacturer planning team on the pre-operative CT scan. (iii) Pre- and post-operative positions were also compared. Longitudinal distance and clock face discrepancies >3 mm and 15°, respectively, were considered significant. Reproducibility was assessed using Bland–Altman and linear regression analysis.

Results: A total of 195 target arteries were analysed. Both Bland–Altman and linear regression showed good reproducibility between the three measurement techniques performed. The median absolute difference between the simulation and post-operative CT scan was 1.0 ± 1.1 mm for longitudinal distance measurements and 6.9 ± 6.1° for clock positions. The median absolute difference between the planning centre and post-operative CT scan was 0.8 ± 0.8 mm for longitudinal distance measurements and 5.1 ± 5.0° for clock positions. Finally, the median absolute difference between the simulation and the planning centre was 0.96 ± 0.97 mm for longitudinal distance measurements and 4.8 ± 3.6° for clock positions.

Conclusion: The numerical model of deployed fenestrated stent grafts is accurate for planning position of fenestrations. It has been validated in 51 patients, for whom fenestration locations were similar to the sizing performed by physicians and the planning centre.

Keywords: Computational analysis, Fenestrated endovascular aneurysm repair, Numerical simulation personalised medicine
Article history: Received 14 April 2019, Accepted 16 October 2019, Available online 19 December 2019

INTRODUCTION

In most high volume European aortic centres, stent graft (SG) implantation is considered the first line treatment for thoracic and abdominal aortic aneurysms (AAAs) in patients with suitable anatomies.[1,2] Fenestrated stent grafting (FEVAR) is a validated endovascular approach to treat complex AAA with unfavourable anatomies (short infrarenal neck, suprarenal or type IV thoraco-abdominal aneurysms).[3–7]

* Corresponding author. 51 Avenue du Maréchal de Lattre de Tassigny, 94010 Créteil, France.
E-mail address: deryckelucie@gmail.com (Lucie Derycke).

https://doi.org/10.1016/j.ejvs.2019.10.009

FEVAR requires custom made devices specifically tailored to each patient's anatomy. As a result, the delay for planning and manufacturing currently ranges from six to eight weeks, which may preclude its use in patients presenting with large aneurysms. Accurate device planning requires the use of dedicated three dimensional imaging software combined with a high resolution pre-operative computed tomography (CT) scan to perform all the necessary measurements. In patients with arterial tortuosity or important angulation, it is difficult to predict SG behaviour in the aorta and to modify the semi-automated arterial segmentation and centreline reconstructions accordingly.

Finite element analysis (FEA) is a numerical method used to overcome biomechanical problems using displacement, strain, and stress analysis.[8] FEA can be used to predict the deployment of SGs in aortic aneurysms.[9–13] Recent literature has highlighted the advances in computational analysis applied to endovascular repair. Based on analyses focused on the mechanical behaviour of SGs,[14] models of EVAR and suprarenal devices deployed in virtual models have been established;[15,16] these patient specific models have proved reliable.[9–13]

The aim of this study was to assess two different steps of a patient specific finite element model of Zenith® fenestrated device deployment in complex AAAs to predict fenestration positions. The primary hypothesis was that simulation would provide accurate positioning of fenestrations compared with standard planning techniques and post-operative CT scan measurements.

MATERIALS AND METHODS

Study population

The study was approved by the Institutional Review Board of the French Society of Thoracic and Cardiovascular Surgery (Société Française de Chirurgie Thoracique et Cardio Vasculaire—SFCTCV).

The study population consisted of 51 consecutive patients who underwent implantation of a Zenith® fenestrated AAA endovascular graft (Cook Medical, Bloomington, IN) to treat juxtarenal, pararenal, or thoraco-abdominal aortic aneurysms between January 2016 and April 2018 at Henri Mondor Hospital and Marie Lannelongue Hospital.

Exclusion criteria were non-availability of pre-operative CT scan, poor pre-operative CT scan quality precluding modelling analysis (poor quality of the contrast agent injection or large slice thickness ($>$ 3 mm)), post-dissection aneurysms, and devices combining branch(es) and fenestration(s).

Sizing process

The sizing of the SG was performed by the manufacturer (Cook Medical®, London, UK).

Simulation strategy

High resolution pre-operative arterial phase CT scans were used to generate patient specific three dimensional (3D) models of the aorta, from the descending thoracic aorta to the common iliac arteries, including the target arteries (coeliac trunk, superior mesenteric, and renal arteries) using the VMTK (Vascular Modeling Toolkit, www.vmtk.org) library. This open source software semi-automatically segments DICOM (Digital Imaging and Communications in Medicine) datasets from the CT scan and creates 3D vascular models (aortic segmentation step).[17] As calcifications of the aortic wall and intraluminal thrombus were not included in the model, the aortic wall and the target vessels were considered as homogeneous surfaces with a constant thickness of 1.5 mm and 1 mm respectively. The custom made SGs were reproduced digitally on the basis of the graft plan data. Deployment of the personalised SG in its corresponding model of the aorta was performed retrospectively using the commercially available Abaqus/Explicit v6.14 finite element solver (Dassault Systèmes, Paris, France). Simulations were achieved using proprietary algorithms (Planop, PrediSurge, Saint-Etienne, France). Computational technology was based on finite element analysis and assessed the deformations induced by the device—host interaction resulting in a prediction of SG behaviour and arterial displacement. Briefly, the aortic surface was virtually deformed until a cylindrical shape of the aorta was obtained. This step of numerical aortic deformation was called "morphing". Then, it was possible to deploy a stent graft inside the cylindrical aorta, and to reverse the deformation of the aortic surface while maintaining the stent graft in place (Fig. 1). The validation of this model was previously reported by the group.[9,10]

The aortic wall was assigned an orthotropic elastic behaviour. Mechanical properties of stents and fabric were obtained either from literature or from in house mechanical testing of samples obtained from manufacturers.[14] For the stents, a linear elastic material behaviour was used, reproducing the nitinol behaviour in its austenitic phase.[14] The polyester fabric was modelled as an orthotropic elastic material.[14]

Simulation analysis

For each visceral artery incorporated into the graft, two data parameters were measured by a blinded investigator: the longitudinal distance between the ostial centres along the centreline, measured in millimetres (mm), and the rotational clock angle between each visceral artery, measured in degrees (°). These two parameters encoded the position of the visceral arteries relative to one another.

Automated fenestration positions were calculated by the software from the "morphing" step.

The different steps of the simulation methodology are illustrated in Fig. 1.

Post-operative images analysis

One trained and independent observer performed the post-operative imaging analysis. The position of the fenestrations on the post-operative CT scan represents the "ideal" SG configuration because any sizing mismatch is compensated

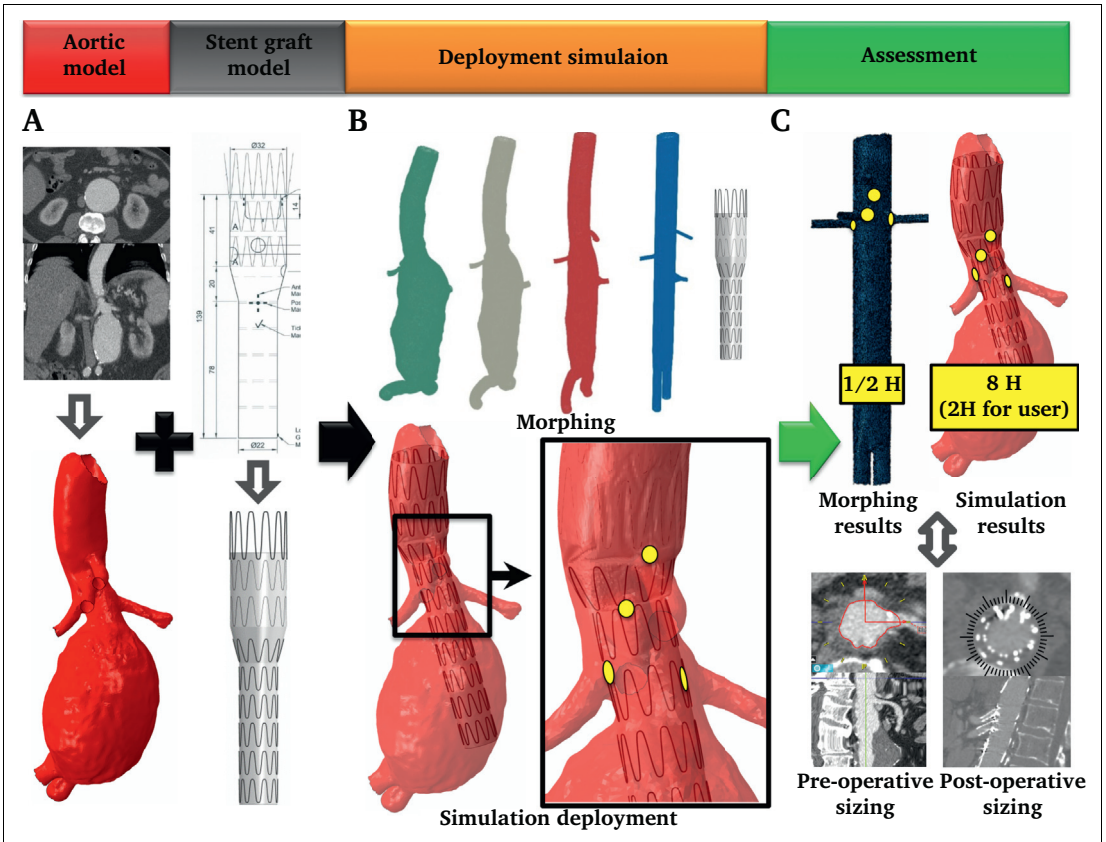

Figure 1. Simulation methodology. (A) Aortic and stent graft modelling (B) "Morphing" step and deployment simulation. (C) Fenestrations positioning on the cylindrical aortic shape and on the deformed graft are compared with standard planning techniques and post-operative computed tomography scan measurements.

by the stent graft's longitudinal (stents are not connected to each other) and rotational (10%—20% oversizing) flexibility. The measures of relative angle and distance between each visceral artery were extracted using a dedicated imaging workstation (TeraRecon Inc., Santa Rosa, CA, USA) and the modality previously described for pre-operative sizing.[18]

Statistical analysis

All statistical analyses were performed using R statistical software version 3.5.2 (R Foundation for Statistical Computing, Vienna, Austria). Unlike the real deployment process, the simulated SG was not deployed inside the aorta based on the position of one of the target arteries but with an automatic longitudinal position and an overall rotation of zero degrees. A systematic measurement bias could have been induced by this method. In order to provide relevant comparisons between the implanted FEVAR and simulation processes, a constant shift was applied to all the fenestrations for each case to correct potential differences induced by these two parameters. However, the relative distances and angles between the fenestrations for each case were preserved, as illustrated in Fig. 2.

The measures were compared with respect to the absolute longitudinal and rotational differences.

Agreement between the different measures was assessed by plotting the difference between each method relative to each other with the limits of agreement ($\pm$ 1.96 standard deviations around the mean difference) as described by Bland and Altman. Quantitative variables were also analysed by linear regression test, used to calculate the bias, estimated by the mean difference and the standard deviation of the difference.

Longitudinal distance and clock face discrepancies $>$ 3 mm and $>$ 15°, respectively, were considered significant, according to the interobserver variability of pre-operative sizing reported in the literature.[18—20]

RESULTS

Fifty-one FEVAR deployments were simulated with a total of 180 fenestrations and 15 scallops (195 target arteries). Details are reported in Table 1. Examples of simulation results are presented in Fig. 3. Fifteen patients were excluded for non-availability of pre-operative CT scan (3/15), poor pre-operative CT scan quality (5/15), post-dissection aneurysms (4/15), and devices combining branch(es) and fenestration(s) (3/15).

In current practice, numerical simulations required approximately eight hours of computational analysis, including two hours of manual work. The automated fenestration positions extracted from the "morphing" step were obtained in approximately half an hour.

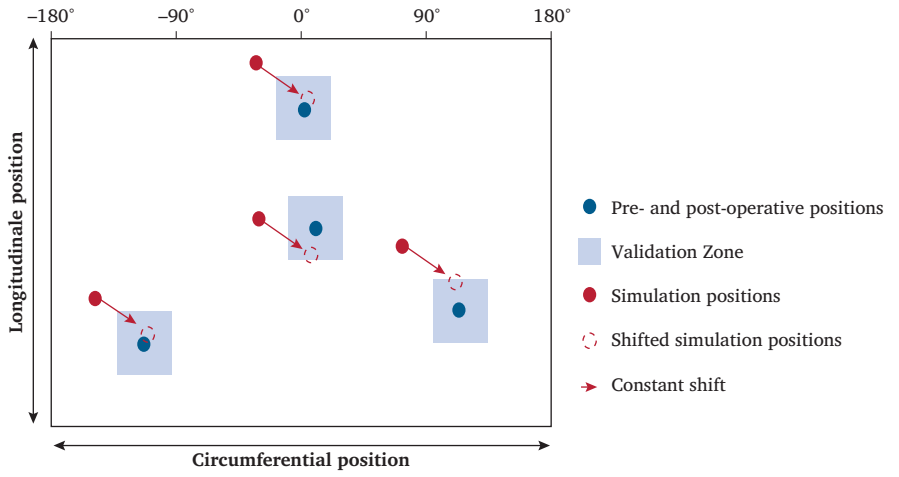

Figure 2. Illustration of constant shift applied on simulation results. The relative distances and angles between the fenestrations for each case are preserved.

The mean slice thickness of the pre-operative CT scans was 1.2 ± 0.45 mm (0.5—2.0). Similar results were obtained when comparing infra- or millimetric CT scans and supra-millimetric CT scans.

Quantitative assessment

The numerical results are summarised in Table 2.

Both Bland—Altman and linear regression showed good reproducibility for longitudinal and circumferential position between the three methods (Fig. 4).

The median absolute difference between the simulation and post-operative CT scan was 1.0 ± 1.1 mm for longitudinal distance measurements and 6.9 ± 6.1° for clock positions. The worst case was a longitudinal distance difference of 6.0 mm and an angle difference of 44.3°. Ninety five per cent of the longitudinal deviances were shorter than 3 mm (43/51 cases) and 96% of the rotational deviances were under 15° (44/51 cases).

The median absolute difference between the planning centre and post-operative sizing was 0.8 ± 0.8 mm for longitudinal distance measurements and 5.1 ± 5.0° for clock positions. The worst case was a longitudinal distance difference of 4.0 mm and an angle difference of 37.1°. Ninety seven per cent of the longitudinal deviances were shorter than 3 mm (46/51 cases) and 98% of the rotational deviances were under 15° (48/51 cases).

The median absolute difference between the simulation and the planning centre was 0.96 ± 0.97 mm for longitudinal distance measurements and 4.8 ± 3.6° for clock positions. The worst case was a longitudinal distance difference of 5.0 mm and an angle difference of 21.8°. Ninety eight per cent of the longitudinal deviances were shorter than 3 mm (47/51 cases) and 99% of the rotational deviances were less than 15° (49/51 cases).

A subgroup analysis focusing on the number of fenestrations (group 1: four fenestrations or scallop (39/51) and group 2: three fenestrations or scallop (11/51)) showed similar results. The median absolute difference between the simulation and the post-operative sizing was approximately 1 mm (1.0 ± 1.2 mm and 1.0 ± 1.2 mm, respectively) for longitudinal distance measurements and 7.5° (7.0 ± 6.3° and 7.9 ± 5.2°, respectively) for clock positions. The median absolute difference between the simulation and the planning centre was approximately 1 mm (0.9 ± 1.2 mm and 1.2 ± 0.9 mm, respectively) for longitudinal distance measurements and 5° (4.8 ± 3.6° and 4.8 ± 3.8°, respectively) for clock positions.

Table 1. Distribution of fenestrations and scallops of the simulated stent grafts

n of fenestrations/ scallops	Cases (*n*)	Fenestrations (*n*)	Scallops (*n*)
5/0	1	5	0
4/0	28	112	0
3/0	7	21	0
4/1	1	4	1
3/1	10	30	10
2/1	4	8	4
Total	51	180	15

Qualitative assessment

Two cases of proximal suboptimal apposition were observed and one case presented with an excess graft oversizing (Fig. 5A,B). An inhomogeneous deployment of the SG was observed in six cases; it was also depicted on the post-operative CT scan. On the example, the posterior stent struts were tightened whereas the anterior struts were spread apart. This stent configuration was similar on the simulation and the post-operative CT scan (Fig. 5C). Two cases presented a SG shifted towards the aortic axis because of a significant misalignment of the aneurysm sac and the aortic axis (Fig. 6). In six cases, pleated fabric was

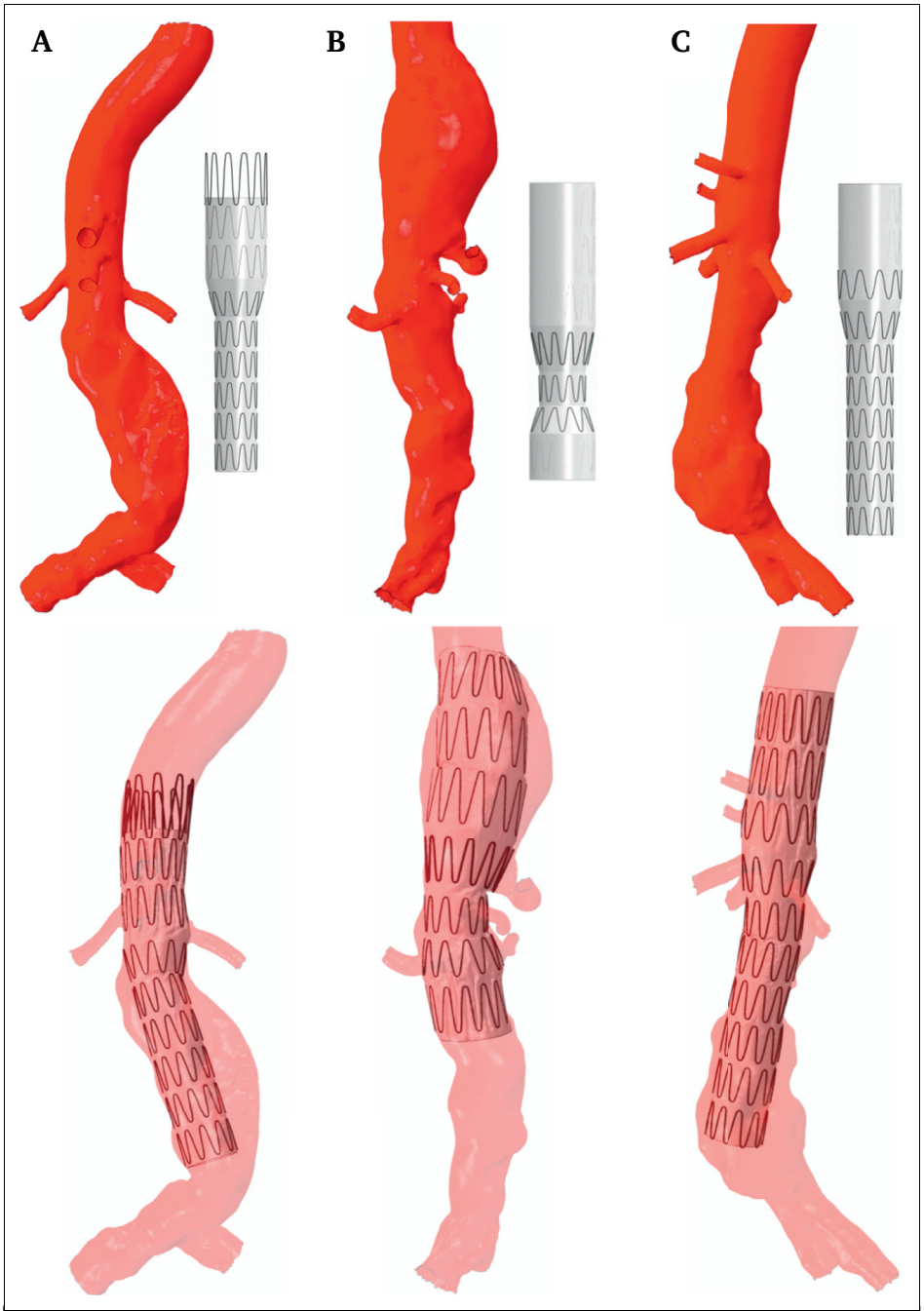

Figure 3. Illustration of the three different stent graft modelling and simulation results. (A) stent graft with proximal bare stent. (B,C) Stent graft without bare stent with two different geometries.

observed at the level of the visceral arteries and a similar aspect was found on the corresponding post-operative CT scan (Fig. 5D,E).

Automated sizing process

The numerical results are summarised in Table 2.

The median absolute difference between automated and post-operative sizing was 3.0 ± 0.3 mm for longitudinal distance measurements and 11.0 ± 9.3° for clock positions. The worst case was a longitudinal distance difference of 16.7 mm and an angle difference of 56.0°. Ninety three per cent of the longitudinal deviances were shorter than 3 mm (39/51 cases) and 91% of the rotational deviances were under 15° (38/51 cases).

The median absolute difference between automated sizing and the planning centre was 1.2 ± 1.7 mm for longitudinal distance measurements and 7.4 ± 6.5° for clock positions. The worst case of each was a longitudinal distance difference of 15.5 mm and an angle difference of 44.9°. Ninety three per cent of the longitudinal deviances were under 3 mm (40/51 cases) and 97% of the rotational deviances were under 15° (46/51 cases).

Table 2. Comparison results of longitudinal and clock positions obtained by the two steps of the simulation model and the pre- and post-operative sizing; and percentage of longitudinal and clock position discrepancies below the significance limits of 3 mm and 15°

	Longitudinal position − mm				Circumferential position − °			
	Post-operative sizing		Pre-operative sizing		Post-operative sizing		Pre-operative sizing	
	Median ± SD (range)	*n*≤3 mm (%)	Median ± SD (range)	*n*≤3 mm (%)	Median ± SD (range)	*n*≤15° (%)	Median ± SD (range)	*n*≤15° (%)
Simulation	1.0 ± 1.1 (−5.9 to 6.0)	95	0.96 ± 0.97 (−4.6 to 5.0)	98	6.9 ± 6.1 (−44.3 to 25.1)	96	4.8 ± 3.6 (−21.8 to 19.3)	99
Pre-operative sizing	0.8 ± 0.8 (−4.0 to 4.0)	97			5.1 ± 5.0 (−37.1 to 18.4)	98		
Automated positions	3.0 ± 0.3 (−9.5 to 16.7)	93	1.2 ± 1.7 (−15.5 to 9.5)	93	11.0 ± 9.3 (−56.0 to 38.0)	91	6.5 ± 6.1 (−44.9 to 34.0)	93

SD = standard deviation.

DISCUSSION

Treatment of complex AAA by FEVAR has been proven feasible, effective and safe[3–7] and has the potential to greatly reduce the mortality and morbidity risks, especially in the subgroup of patients at high risk of open repair. However, the use of fenestrated devices implies proper analysis of the arterial geometry to design a custom made SG. Physicians have to be trained to use dedicated sizing

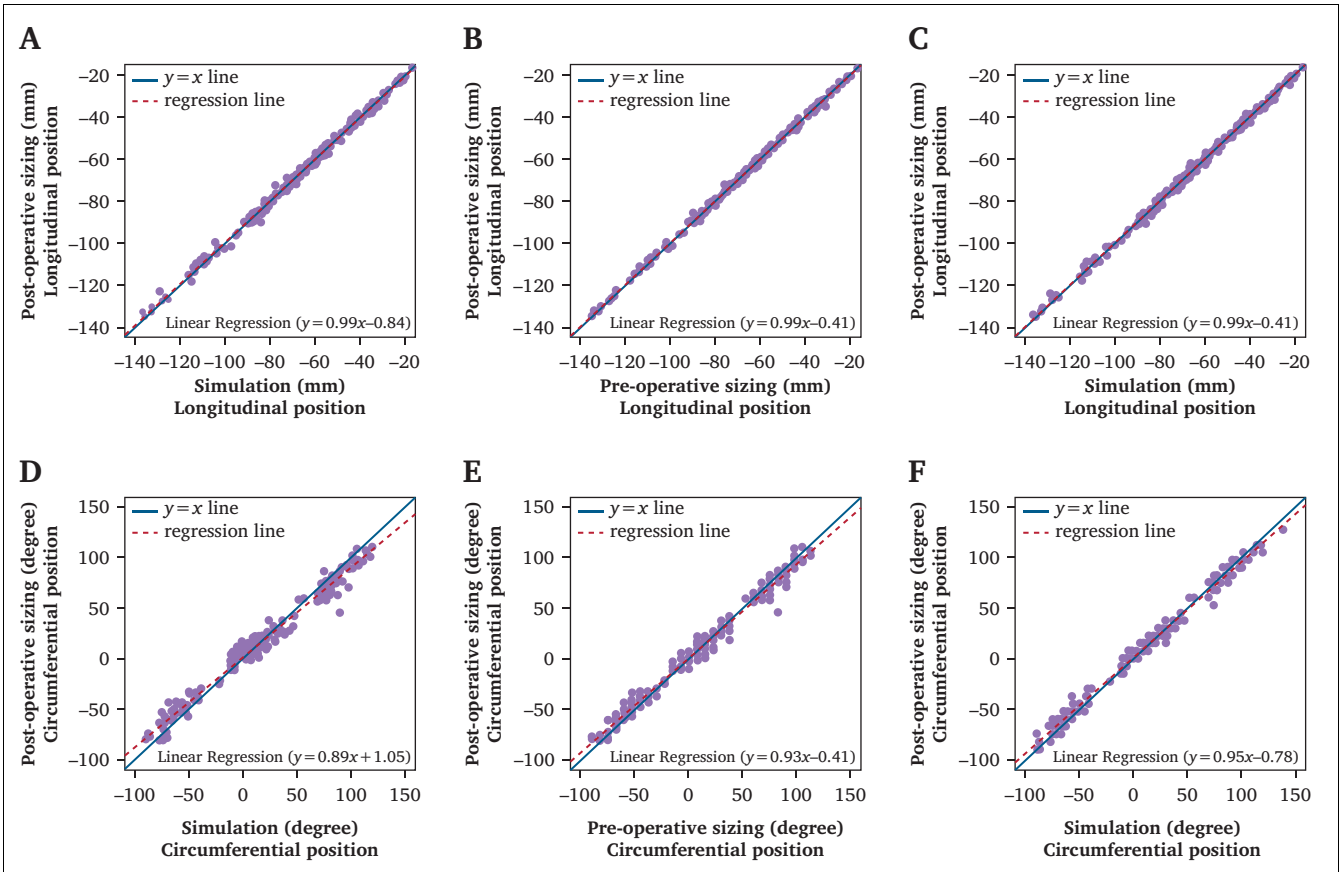

Figure 4. Longitudinal and clock position of target vessels shown with the simulation and the pre- and post-operative measurements. The comparison is performed by linear regression analysis. (A–C) Comparison of longitudinal positions extracted from simulation and post-operative sizing (A), from pre- and post-operative sizing (B), and from simulation and pre-operative sizing (C). (D–F) Comparison of circumferential positions extracted from simulation and post-operative sizing (D), from pre- and post-operative sizing (E), and from simulation and pre-operative sizing (F).

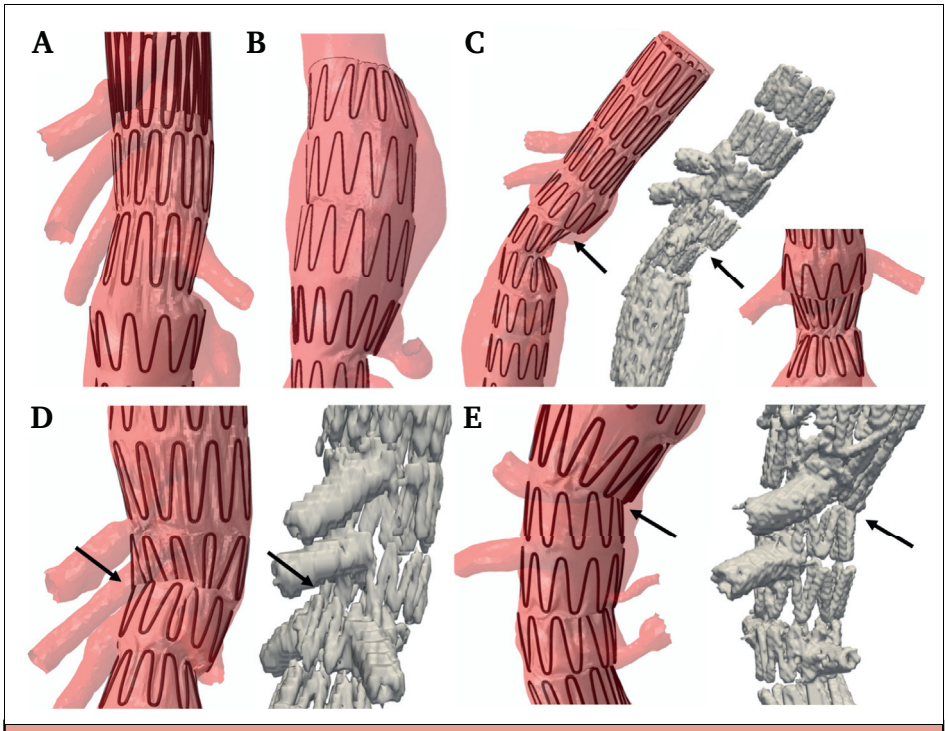

Figure 5. Qualitative assessment examples. (A) Oversizing excess; (B) defect of proximal apposition; (C) case of inhomogeneous stent graft deployment: simulation (in red) is compared with a similar view of the implanted stents extracted from the post-operative computed tomography (CT) scan (in grey); left lateral and posterior views. (D,E) Anterior view of two cases with a pleated fabric on simulations results (in red) and comparison with similar view of the actual stents extracted from the post-operative CT scan (in grey).

software and to be familiar with 3D imaging and its limitations.[21,22] An automated, reproducible and precise sizing procedure could facilitate the clinical process and free up physician time.

The model proved successful in providing fenestration locations similarly to the current sizing performed by the planning centre, confirmed by the comparison with the post-operative analysis. The process has been successfully evaluated in 51 patients.

Accurate positioning of the fenestrations is a determinant of procedural success and long term patency. Numerical simulation of SG deployment offers other potential advantages. The behaviour of the deployed SG can be visualised and assessed, including adequate application of the fabric, proximal apposition, excessive oversizing or kinking, as seen in Fig. 5. These results indicate the clinical relevance of numerical simulation of FEVAR to improve outcome by helping the physician to select appropriate graft diameters and fenestration positions that best fits the individual patient. In unfavourable aortic anatomies, a deployment simulation could be performed by the planning centre to accept or reject cases. To allow relevant comparison, an accurate digital reproduction of patient specific SGs was performed based on the graft plan data. Standardised digital SG models are currently being constructed to provide a quick and easy to use interface.

In less than 15% of cases longitudinal and rotational differences greater than 3 mm or 15° were recorded. There is no consensus regarding maximum tolerance level between fenestrations and target vessels positions. Some experienced endovascular specialists suggested that a rotational deviance of 15° between the fenestration and its target vessel was acceptable, as it was unlikely to lead to significant complications.[23] The results confirm the previous studies focused on interobserver variability when sizing FEVAR, which reported good agreement but also some critical discrepancies between observers. Oshin *et al.* reported an analysis of 25 FEVAR sizings performed by two experienced operators; they observed deviances of more than 3 mm in longitudinal position in 18% of cases, and of more than 15° in 12% of cases on clock position.[20] Banno *et al.*[18] reported a comparison of 268 FEVAR sizings between two experienced surgeons and the manufacturer. They observed more than 22.5° angle discrepancy in 9.8% of cases and more than 5 mm length discrepancy in 16.4% of cases. Finally, Malkawi *et al.*[19] reported results of a comparison of 19 FEVAR sizings among four experienced observers. The overall interobserver measurement error for distance was 5.3 mm (95% confidence interval (CI) 4.4—6.2) and for target vessel orientation 12.6° (95% CI 10.8—14.4). Maurel *et al.*[24] reported a comparison of FEVAR pre- and post-operative sizing of renal artery distance and clock position and showed that an accommodation to sizing error up to 15° in clock position may be considered acceptable, without adverse consequences on patency. The current results compare favourably with these data.

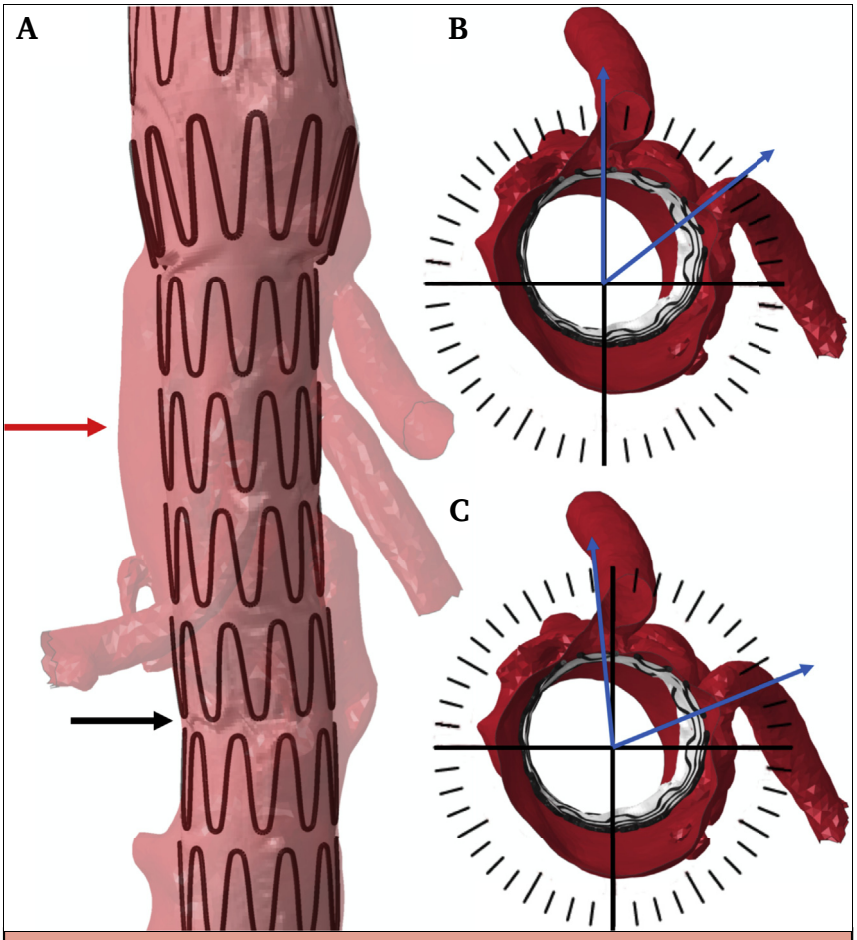

Figure 6. Challenging clock position analysis. (A) Right lateral view; red arrow, the stent graft has shifted forwards in the aortic lumen; black arrow, the stent graft is constrained by the previously implanted endovascular abdominal aortic aneurysm repair. Transverse views of (B) superior mesenteric and right renal arteries clock positions with the clock aligned with the aortic lumen centreline and (C) with the clock aligned with the stent graft lumen centreline.

Furthermore, discrepancies could be partly explained by the adjustment of the fenestrations designed by the manufacturer to fit with the 15%—20% graft oversizing, the presence of reducing ties, and fenestration shift to avoid having a stent strut crossing the lumen of a fenestration. These rotational adjustments explain why longitudinal measurements showed less variability than circumferential measurements. The technique of clock position measurement, with its 7.5° accuracy, compared with the 1 mm accuracy of longitudinal measurements, also explains this difference.

A thorough examination of the cases has identified causes of discrepancy. An inhomogeneous deployment of the SG was observed in six cases associated with rotational position misalignment, which was also found on the postoperative CT scan (Fig. 5). In misalignment of the aneurysmal sac and aortic axis, the SG was shifted away from the aortic axis, especially in cases with prior EVAR. In Fig. 6, one of these cases is presented: the SG, which is constrained above and below the aneurysm, is shifted forward in the aortic lumen at the level of the aneurysm. Different clock positions are obtained depending on whether the aortic lumen axis or the SG axis is used as a reference. In six cases with a longitudinal position misalignment, pleated fabric was observed at the level of the visceral arteries and a similar aspect was found on the corresponding postoperative CT scan, as shown in Fig. 5. Finally, discrepancies were shown in two cases with a large distance between the SG and the visceral artery ostium and three cases with large visceral artery diameter ($>$ 10 mm). In such anatomies, accuracy is less crucial to achieve technical success.

The delay in producing a fenestrated device is related to both planning and manufacturing. The current eight week delay is inappropriate for urgent patients. Nowadays numerical simulations require approximately eight hours of computational analysis, including two hours of manual work, which is similar to the time spent for planning by a trained operator. To further reduce the delay and provide an accurate and fast tool to physicians, computing capabilities

improve at a very rapid pace. In the near future, it is likely that the time required to perform these simulations will fall below an hour.

The first step of the deployment simulation provides visceral artery positions within half an hour. However, the aortic segmentation was inaccurate in some cases with arterial calcification, previous EVAR with struts in front of visceral arteries and ostial stenosis. For such cases, checking the aortic segmentation is still required. A previous study highlighted the need for "human input" in automated sizing for EVAR.[25] Measurement accuracy appeared to be better in the current study, probably due to the improved quality of the CT scans.

This study has several limitations. The study focused on fenestrated devices and non-dissected aortas. Branched device modelling is currently feasible and will be assessed in specific studies. Improvements are also in progress to extend the model to dissected aortas. Moreover, the study focused on the Zenith Cook Medical device because it is the most commonly implanted fenestrated endograft in both centres, and because the position of the fenestration is critical on this device, which is fully supported with stents. Simulation of other fenestrated devices, which require different planning methods, will be performed in a separate study. The simulations could benefit from more sophisticated modelling, including thrombus, and aortic wall calcification and environment. Current validation of simulation models remains a major issue. Simulation results were compared with pre- and post-operative sizing, which have their own limitations, and CT images analysis and numerical models of SG deployment were performed retrospectively.

Numerical simulation of SG deployment in complex AAAs was feasible in 51 patients and accurately determined patient specific fenestration positions. When compared with post-operative sizing, the current process of sizing achieved by the planning centre showed less variability than the simulation model and automated positions extracted directly from the "morphing" step still required manual corrections. It is currently being improved with new computational algorithms. This model is a reliable tool for FEVAR planning and has the potential to help physicians select the device design that best fits the patient's aortic anatomy. Evaluation of the software in other conditions, such as unsuccessful cases, high arterial tortuosity cases and physician modified stent grafts, should be addressed in further studies. Moreover, prospective work should be done in order to support these promising early results.

CONFLICT OF INTEREST

J.N. Albertini, D. Perrin, and S. Avril are cofounders of the company PrediSurge SAS. S. Haulon is consultant for Cook Medical. F. Cochennec is proctor for Cook Medical. The other authors have no conflict of interest.

FUNDING

None.

REFERENCES

1 Wanhainen A, Verzini F, Van Herzeele I, Allaire E, Bown M, Cohnert T, et al. Editor's choice - European Society for Vascular Surgery (ESVS) 2019 clinical practice guidelines on the management of abdominal aorto-iliac artery aneurysms. *Eur J Vasc Endovasc Surg* 2019;**57**:8–93.

2 Riambau V, Böckler D, Brunkwall J, Cao P, Chiesa R, Coppi G, et al. Editor's choice - management of descending thoracic aorta diseases: clinical practice guidelines of the European Society for Vascular Surgery (ESVS). *Eur J Vasc Endovasc Surg* 2017;**53**:4–52.

3 Mastracci TM, Eagleton MJ, Kuramochi Y, Bathurst S, Wolski K. Twelve-year results of fenestrated endografts for juxtarenal and group IV thoracoabdominal aneurysms. *J Vasc Surg* 2015;**61**:355–64.

4 Marzelle J, Presles E, Becquemin JP. WINDOWS trial participants. Results and factors affecting early outcome of fenestrated and/or branched stent grafts for aortic aneurysms: a multicenter prospective study. *Ann Surg* 2015;**261**:197–206.

5 Verhoeven ELG, Vourliotakis G, Bos WTGJ, Tielliu IFJ, Zeebregts CJ, Prins TR, et al. M. Fenestrated stent grafting for short-necked and juxtarenal abdominal aortic aneurysm: an 8-year single-centre experience. *Eur J Vasc Endovasc Surg* 2010;**39**:529–36.

6 Oderich GS, Greenberg RK, Farber M, Lyden S, Sanchez L, Fairman R, et al. Results of the United States multicenter prospective study evaluating the Zenith fenestrated endovascular graft for treatment of juxtarenal abdominal aortic aneurysms. *J Vasc Surg* 2014;**60**:1420–8. e1–5.

7 British Society for Endovascular Therapy and the Global Collaborators on Advanced Stent-Graft Techniques for Aneurysm Repair (GLOBALSTAR) Registry. Early results of fenestrated endovascular repair of juxtarenal aortic aneurysms in the United Kingdom. *Circulation* 2012;**125**:2707–15.

8 Leach JR, Mofrad MRK, Saloner D. Computational models of vascular mechanics [Internet]. In: *Computational modeling in biomechanics*. Dordrecht: Springer Netherlands; 2010. p. 99–170.

9 Perrin D, Badel P, Orgeas L, Geindreau C, du Roscoat SR, Albertini J-N, et al. Patient-specific simulation of endovascular repair surgery with tortuous aneurysms requiring flexible stent-grafts. *J Mech Behav Biomed Mater* 2016;**63**:86–99.

10 Perrin D, Badel P, Orgéas L, Geindreau C, Dumenil A, Albertini J-N, et al. Patient-specific numerical simulation of stent-graft deployment: validation on three clinical cases. *J Biomech* 2015;**48**:1868–75.

11 Auricchio F, Conti M, Marconi S, Reali A, Tolenaar JL, Trimarchi S. Patient-specific aortic endografting simulation: from diagnosis to prediction. *Comput Biol Med* 2013;**43**:386–94.

12 Romarowski RM, Conti M, Morganti S, Grassi V, Marrocco-Trischitta MM, Trimarchi S, et al. Computational simulation of TEVAR in the ascending aorta for optimal endograft selection: a patient-specific case study. *Comput Biol Med* 2018;**103**:140–7.

13 Derycke L, Perrin D, Cochennec F, Albertini J-N, Avril S. Predictive numerical simulations of double branch stent-graft deployment in an aortic arch aneurysm. *Ann Biomed Eng* 2019.

14 Demanget N, Avril S, Badel P, Orgéas L, Geindreau C, Albertini J-N, et al. Computational comparison of the bending behavior of aortic stent-grafts. *J Mech Behav Biomed Mater* 2012;**5**:272–82.

15 Perrin D, Demanget N, Badel P, Avril S, Orgéas L, Geindreau C, et al. Deployment of stent grafts in curved aneurysmal arteries: toward a predictive numerical tool. *Int J Numer Methods Biomed Eng* 2015;**31**:e02698.

16 De Bock S, Iannaccone F, De Beule M, Vermassen F, Segers P, Verhegghe B. What if you stretch the IFU? A mechanical insight into stent graft Instructions For Use in angulated proximal aneurysm necks. *Med Eng Phys* 2014;**36**:1567–76.

17 Sethian JA. A fast marching level set method for monotonically advancing fronts. *Proc Natl Acad Sci U S A* 1996;**93**:1591–5.

18 Banno H, Kobeiter H, Brossier J, Marzelle J, Presles E, Becquemin J-P. Inter-observer variability in sizing fenestrated and/or branched aortic stent-grafts. *Eur J Vasc Endovasc Surg Off J Eur Soc Vasc Surg* 2014;**47**:45–52.
19 Malkawi AH, Resch TA, Bown MJ, Manning BJ, Poloniecki JD, Nordon IM, et al. Sizing fenestrated aortic stent-grafts. *Eur J Vasc Endovasc Surg* 2011;**41**:311–6.
20 Oshin OA, England A, McWilliams RG, Brennan JA, Fisher RK, Vallabhaneni SR. Intra- and interobserver variability of target vessel measurement for fenestrated endovascular aneurysm repair. *J Endovasc Ther* 2010;**17**:402–7.
21 Moore R, Hinojosa CA, O'Neill S, Mastracci TM, Cinà CS. Fenestrated endovascular grafts for juxtarenal aortic aneurysms: a step by step technical approach. *Catheter Cardiovasc Interv* 2007;**69**:554–71.
22 Greenberg RK, West K, Pfaff K, Foster J, Skender D, Haulon S, et al. Beyond the aortic bifurcation: branched endovascular grafts for thoracoabdominal and aortoiliac aneurysms. *J Vasc Surg* 2006;**43**:879–86. discussion 886-887.
23 Nordon IM, Hinchliffe RJ, Manning B, Ivancev K, Holt PJ, Loftus IM, et al. Toward an "off-the-shelf" fenestrated endograft for management of short-necked abdominal aortic aneurysms: an analysis of current graft morphological diversity. *J Endovasc Ther* 2010;**17**:78–85.
24 Maurel B, Lounes Y, Amako M, Fabre D, Hertault A, Sobocinski J, et al. Changes in renal anatomy after fenestrated endovascular aneurysm repair. *Eur J Vasc Endovasc Surg* 2017;**53**:95–102.
25 Wyss TR, Dick F, England A, Brown LC, Rodway AD, Greenhalgh RM. Three-dimensional imaging core laboratory of the endovascular aneurysm repair trials: validation of methodology. *Eur J Vasc Endovasc Surg* 2009;**38**:724–31.